An Efficient Polarization Converter for Mid-IR Wavelength

Ajanta Barh,[1] B. M. A. Rahman,[2] R. K. Varshney,[1] and Bishnu P. Pal[1]
[1]Department of Physics, Indian Institute of Technology Delhi, New Delhi, India
[2]School of Engineering and Mathematical Sciences, City University London, London, UK
e-mail: bppal@physics.iitd.ernet.in

Abstract: Design of a silicon-based polarization converter through phase matched power coupling between TE and TM modes is presented. Conversion efficiency up to 90% is feasible at 3 µm wavelength with device length of 536 µm.

OCIS codes: (040.6040) Silicon; (230.7370) Waveguides; (230.3120) Integrated optics devices; (130.5440) Polarization-selective devices; (000.4430) Numerical approximation and analysis.

1. Introduction

By drawing parallel to chip level integration that brought in cost reduction in electronics it is conceivable that for attaining similar gains in optoelectronics, which is not limited by electronic speed, one would need to make the devices as small as possible and find a material system for monolithic integration of all components. One plausible route would be to reduce the device size through use of high refractive index (RI) contrast waveguides (WG), which can improve the optical confinement and effectively reduce the waveguide dimensions.

Silicon-on-insulator (SOI) [1] can provide large refractive index contrast between Si core and silica cladding (~ 3). It is emerging as a low-cost technology by integrating it directly on top of a well developed CMOS platform [2, 3]. Today, Si-based platforms support a wide variety of devices, including high-speed modulators and detectors [4], low-loss waveguides with passive and active [5], linear and non-linear [6] components.

Typically, light output from a conventional fiber often used as input to an integrated optical chip is randomly polarized. State of polarization (SOP) of light has a great impact on both photonic circuit design and operation. On the other hand, though the Si WG dimensions are small, they are highly polarization sensitive. Thus, for polarization diversity systems, the problem can be sorted out by incorporating polarization splitter and polarization converter based on such WGs. A variety of polarization converters (PC) have been proposed in recent years [7-9]. In all these cases either the device design is simple but conversion efficiency is poor or the conversion efficiency is good but the device design is complex.

In this paper, we propose design for realizing a PC for potential application at the mid-IR wavelength region that should be relatively easy to fabricate as uniform cross section is maintained along length and the whole structure, made out of two WGs (one Si strip WG and one Si vertical slot WG [10]), can be made with a single mask. Moreover, it can rotate both polarization states for a single input direction (i.e., at coupling length (L_c), TM input in the Si strip WG will produce TE output from the slot WG and TE input in the slot WG will produce TM output from the strip WG). We have optimized the design and shown that maximum power coupling efficiency (C_m) > 90% is possible for a device length of 535.8 µm. Device performance is also studied on the basis of fabrication tolerances.

2. Methodology

For high RI contrast WGs, where the modal hybridness is very strong, the full-vectorial mode solver is essential. For our design a full vectorial finite element method (FV-FEM) was implemented to analyze the 2-D structure. All the vector fields are investigated and depending on modal hybridness, TE and TM modes are identified. Based on this FV-FEM the polarization beat length is calculated. Propagation of these two orthogonal modes is studied by "Eigenmode Expansion" method using the commercially available FIMMPROP software. Here we have launched TE-like and TM-like mode as the input at respective WGs and studied the power propagation along its length.

Our proposed PR is a coupler based on one Si-strip WG and one Si-air vertical slot WG. The cross-section is shown in Fig. 1(a). Here two WGs are implemented on silica (SiO_2) as the substrate with air as cover and slot material. We have taken the same height for both the WGs as H and same width for the high index regions of the slot WG as W_2. The width of the strip WG core and low index region of slot WG are taken as W_1 and W_S, respectively. The separation between two WGs is denoted as S. Our working wavelength is 3.0 µm, for which the refractive indices of Si and SiO_2 are 3.43232 and 1.41925, respectively. Note that both Si and SiO_2 (fused silica IR grades [11]) are transparent at this wavelength. A vertical slot WG will only support a quasi-TE mode, which has E_x as the dominant E-field component. So, here confinement of the fundamental TE mode in slot and TM mode in strip WG is considered. For moderate electric field confinement in the slot, we choose W_S as 100 nm. Maintaining low footprint along with sufficient mode confinement, we have optimized and fixed the H of both WGs as 500 nm for 3 μm wavelength. On the other hand, to maintain TE polarization as the fundamental mode, W_2 needed to be > 500 nm. Optimizing the confinement loss, W_2 was chosen to be 550 nm for H = 500 nm of the slot WG.

3. **Results and Discussions**

Optimized slot WG dimensions are W_2 = 550 nm, W_S = 100 nm, H = 500 nm. In the absence of strip WG, the n_{eff} of the TE mode in this slot WG is 1.85627. Then n_{eff} of the fundamental TM mode inside the isolated strip WG of same H is studied by varying its width (W_1). For W_1 = 992 nm, n_{eff} of strip mode becomes equal to that of the slot WG mode. Then for the combined coupled structure, using these optimized dimensions (i.e. W_1 = 992 nm, W_2 = 550 nm, W_S = 100 nm, H = 500 nm), the phase matching separation between these two WGs was found to be ~ 876 nm.

The three basic parameters to study a PC are n_{eff}, hybridness and coupling length (L_c). For three different S values (800 nm, 900 nm, 1000 nm), the variation of above-mentioned parameters were studied as a function of strip WG width (W_1), shown in Figs. 1(b), 1(c) and 1(d). In Fig. 1(b), horizontal line represents n_{eff} -TE in the slot (almost constant). Slanted line represents n_{eff} -TM in strip WG, changing as W_1 is increased. The anti-crossing point corresponds to the phase matching W_1. Hybridness of the two modes can be defined as the ratio of the maximum values of the H_y to H_x field components for the TM and similarly H_x/H_y for the TE mode. Around this anti-crossing point the mode mixing is maximum leading to higher hybridness. For quasi-TM mode, the variation of hybridness is shown in Fig. 1(c). Similar results can be obtained for TE mode also. Polarization coupling length of the two modes are defined as ($L_c = \pi / |\beta_1 - \beta_2|$) where, β_1 and β_2 are the propagation constants of the TE and TM modes. The peak L_c value (Fig. 1(d)) appears at mode exchange regime but decreases with S. So, smaller S corresponds to smaller footprint of the device. However it brings down the maximum conversion efficiency (C_m). Thus there is a trade-off between smaller device length (L) and C_m. To achieve > 90% conversion, the minimum S would be ≈ 600 nm for which phase matching W_1 and L_c becomes 985 nm and 535.8 μm, respectively. We have therefore focused our further study for S = 600 nm.

The supermodes of this designed PC are shown in Figs. 1(e) and 1(f), where H_x and H_y fields of the dominating TE mode in the slot WG are displayed, respectively. Fig. 1(e) clearly indicates that H_x is in the strip region, which supported the interacting TM mode. Small amount of H_x in slot indicates the high modal hybridness. Fig. 1(f) shows the H_y field of the same supermode, which is the dominating TE mode in slot WG. This is the even supermode of the whole structure as both the signs of H_x and H_y are positive. The other supermode is not shown here.

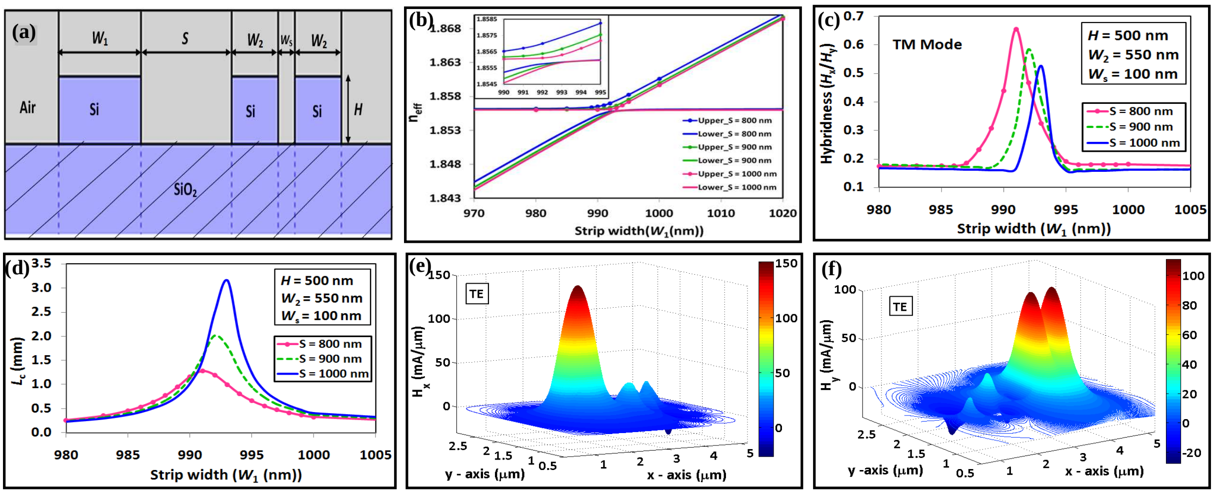

Fig. 1: (a) Schematic transverse view of the proposed polarization converter; (b) Variation in n_{eff} with W_1 for the upper & lower WGs for S = 800 nm, 900 nm and 1000 nm; (c) Variation of modal hybridness of the TM mode with W_1; (d) Variation of coupling length (L_c) with W_1; (e) $H_x(x,y)$ plot of dominating TE mode in slot WG for optimum structure (W_1 = 985 nm, S = 600 nm, W_2 = 550 nm, W_S = 100 nm, and H = 500 nm); (f) $H_y(x,y)$ plot of dominating TE mode in slot WG for optimum structure.

Propagation of TE and TM modes along the device is studied by launching the TE-like mode in slot WG and TM-like mode in strip WG. Assuming TE-like input in slot WG, the intensity variations of TE mode in slot and TM mode in strip WG are shown in Fig. 2(a). Variation of normalized power (P_N) along propagation length is shown for these two modes in Fig. 2(b). It can be clearly seen from these two figures that the total power of input TE mode gets transferred to TM mode at a device length of 535.8 μm, which is nothing but the L_c corresponding to these two modes. Maximum P_N coupled from input TE to output TM mode for this case is ~ 90.4%.

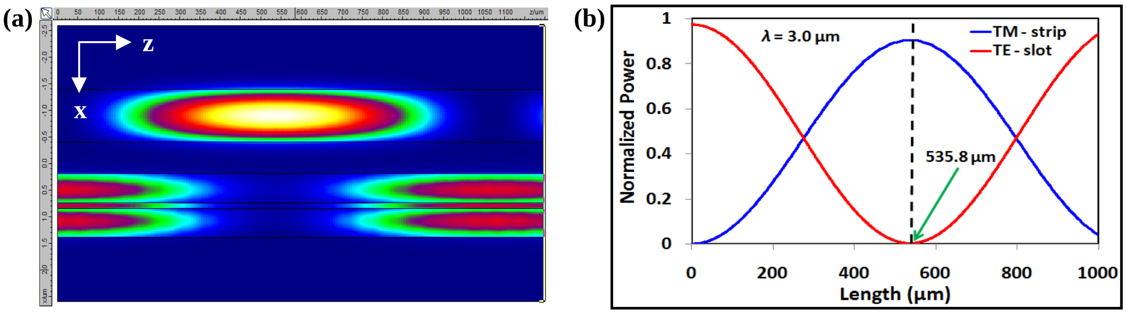

Fig. 2: (a) Intensity variation along device length of TE mode in the slot WG and TM mode in the strip WG for TE-like input in the slot WG; (b) Normalized power variation along the device length of TE mode in the slot WG (Red curve) and TM mode in the strip WG (Blue curve).

From potential fabrication point of view, we have also studied the tolerance of the structure by varying some of the WG parameters like, W_1 by ± 5 nm and W_2, W_s by ± 2 nm and shown the variations in Figs. 3(a), 3(b) and 3(c), respectively. In general, CMOS fabrication technology has significantly better control over height, so only the effect of variation in its width is studied here. The figures reveal that, slot WG parameters are more crucial. However, it may be possible to correct fabrication tolerances by post-trimming of the WGs or temperature tuning.

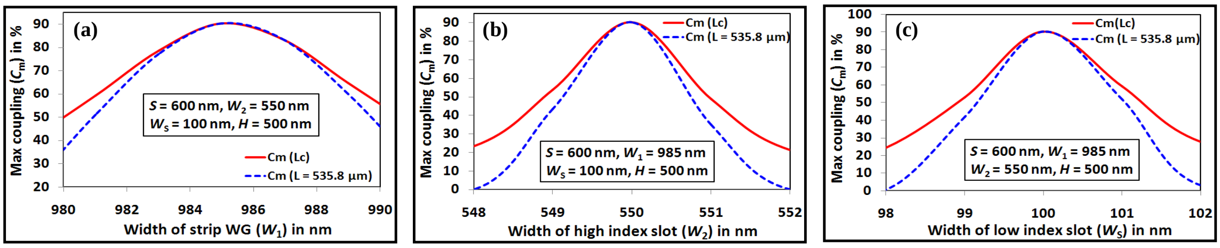

Fig. 3: (a) Tolerance study for W_1; (b) Tolerance study for W_2; (c) Tolerance study for W_s; In all the figures, red solid curve corresponds to C_m at L_c and blue dashed curve corresponds to C_m at device length (L = 535.8 µm).

4. Conclusions and Acknowledgment

A novel design of a compact polarization converter exploring Si photonics is presented. The above results suggests that an appreciably short 535.8 µm long PC can be designed for 3.0 µm wavelength by exploiting the phase matching between the orthogonally polarized modes of a Si-strip WG and Si-air vertical slot WG. Maximum power coupling efficiency > 90% is possible from input TE to output TM mode and vice versa.

Author A.B. gratefully acknowledges the Council of Scientific and Industrial Research (CSIR) for providing her Ph.D. fellowship. This work was partially supported by US Department of the Navy Grant N62909-10-1-7141 issued by Office of Naval Research Global. The United States Government has royalty-free license throughout the world in all copyrightable material contained herein.

5. References

[1] W. Bogaerts, D. Taillaert, B. Luyssaert, P. Dumon, J. Van Campenhout, P. Bienstman, D. Van Thourhout, R. Baets, V. Wiaux, and S. Beckx, "Basic structures for photonic integrated circuits in silicon-on-insulator," Opt. Exp. **12**, 1583-1591 (2004).

[2] L. Tsybeskov, D. Lockwood, and M. Ichikawa, "Silicon photonics: CMOS going optical," in Proc. of the IEEE, 1161-1165 (2009).

[3] B. P. Pal, "Guided-wave optics on silicon: Physics, technology, and status," Progress in Optics **32**, 1-59 (1993).

[4] T. B. Jones, M. Hochberg, G. Wang, R. Lawson, Y. Liao, P. A. Sullivan, L. Dalton, A. K. Y. Jen, and A. Scherer, "Optical modulation and detection in slotted silicon waveguides," Opt. Exp. **13**, 5216-5226 (2005).

[5] P. Pintus, S. Faralli, and F. Di Pasquale, "Low-threshold pump power and high integration in Al_2O_3: Er^{3+} slot waveguide lasers on SOI," IEEE Photonics Technology Lett. **22**, 1428-1430 (2010).

[6] R. M. Osgood, Jr., N. C. Panoiu, J. I. Dadap, X. Liu, X. Chen, I-Wei Hsieh, E. Dulkeith, W. M. Green, and Y. A. Vlasov, "Engineering nonlinearities in nanoscale optical systems: Physics and applications in dispersion-engineered silicon nanophotonic wires," Advances in Optics and Photonics **1**, 162–235 (2009).

[7] N. N. Feng, R. Sun, J. Michel, and L. C. Kimerling, "Low-loss compact-size slotted waveguide polarization rotator and transformer," Opt. Lett. **32**, 2131-2133 (2007).

[8] M. Komatsu, K. Saitoh, and M. Koshiba, "Design of miniaturized silicon wire and slot waveguide polarization splitter based on a resonant tunneling," Opt. Exp. **17**, 19225–19234 (2009).

[9] D. M. H. Leung, B. M. A. Rahman, and K. T. V. Grattan, "Numerical analysis of asymmetric silicon nanowire waveguide as compact polarization rotator," IEEE Photonics Journal. **3**, 381-389 (2011).

[10] V. R. Almeida, Q. Xu, C. A. Barrios, and M. Lipson, "Guiding and confining light in void nanostructure," Opt. Lett. **29**, 1209-1211 (2004).

[11] www.ispoptics.com/PDFs/PDFCatalog/Page16.pdf